Dynamic Spin-Triplet Order Induced by Alternating Electric Fields in Superconductor-Ferromagnet-Superconductor Josephson Junctions

I. V. Bobkova,[1,2,3] A. M. Bobkov,[1] and M. A. Silaev[4,2,5]
[1]*Institute of Solid State Physics, Chernogolovka, Moscow region, 142432 Russia*
[2]*Moscow Institute of Physics and Technology, Dolgoprudny 141700, Russia*
[3]*National Research University Higher School of Economics, Moscow 101000, Russia*
[4]*Department of Physics, Nanoscience Center, University of Jyväskylä, 40014 Jyväskylä, Finland*
[5]*Institute for Physics of Microstructures, Russian Academy of Sciences, 603950 Nizhny Novgorod, GSP-105, Russia*

(Received 27 March 2021; accepted 1 September 2021; published 30 September 2021)

Dynamic states offer extended possibilities to control the properties of quantum matter. Recent efforts are focused on studying the ordered states which appear exclusively under the time-dependent drives. Here, we demonstrate a class of systems which feature dynamic spin-triplet superconducting order stimulated by the alternating electric field. The effect is based on the interplay of ferromagnetism, interfacial spin-orbital coupling, and the condensate motion driven by the field, which converts hidden static p-wave order, produced by the joint action of the ferromagnetism and the spin-orbital coupling, into dynamic s-wave equal-spin-triplet correlations. We demonstrate that the critical current of Josephson junctions hosting these states is proportional to the electromagnetic power, supplied either by the external irradiation or by the ac current source. Based on these unusual properties we propose the scheme of a Josephson transistor which can be switched by the ac voltage and demonstrates an even-numbered sequence of Shapiro steps. Combining the photoactive Josephson junctions with recently discovered Josephson phase batteries we find photomagnetic SQUID devices which can generate spontaneous magnetic fields while being exposed to irradiation.

DOI: 10.1103/PhysRevLett.127.147701

Weak links between two superconducting electrodes known as the Josephson junctions (JJ) are the cornerstone elements of superconducting electronics. For decades there has been an intensive search of technologies and physical principles allowing for the construction of superconducting transistors based on the JJ circuits with controllable switching between superconducting and resistive states [1]. Such devices are expected to pave the way for energy-saving superconducting computers [2]. Recently the interest to JJs with electrically tunable critical currents has been stimulated by the perspectives of applying such systems in leading-edge quantum information architectures [3,4]. Main efforts in this field have been focused on the systems with Josephson currents controlled by electrostatic gates. This concept has been realized in mesoscopic systems with normal metal interlayers [5–10], semiconducting interlayers [1,3,4,11,12] and quantum dots [13,14]. Electrostatic control with constant gate voltages is not enough for most of the applications implying transistors operating under the action of high-frequency drives. Therefore it is of crucial importance to go beyond the electrostatic gating and find the physical mechanisms which could provide a dynamical switching of Josephson junctions by application of a high-frequency electric field.

Here, we suggest a qualitatively different way to controlling the Josephson current using dynamic triplet superconducting states driven by the external time-dependent electric field $\boldsymbol{E}(t)$. This mechanism can help to achieve switching rates in the terahertz and even the visible light frequency domains. It is based on the peculiar quantum state of matter which arises under the nonequilibrium conditions due to the interplay of Rashba-type [15–17] interfacial spin-orbital coupling (SOC), ferromagnetism and oscillating motion of Cooper pairs driven by the alternating electric field. The first two ingredients acting together provide partial conversion of singlet correlations to p-wave equal-spin-triplet correlations, which do not manifest themselves in the diffusive system due to impurity averaging. The last ingredient converts these "hidden" static p-wave to dynamic s-wave equal-spin-triplet correlations via the Doppler shift mechanism. The *triplet* nature of the proposed light-induced dynamical correlations provides an additional advantage opening a perspective of photon-magnon coupling mediated by the triplet correlations. The proposed effect extends the possibilities of generating and controlling nonequilibrium states of matter which have attracted significant attention recently, such as Floquet topological insulators [18], odd-frequency superconductivity [19], time crystals [20–22], driven Dirac materials [23–25], light-induced and light-manipulated superconductivity [26–32], vortex states [33,34], cavity-enhanced ferroelectric phase transition [35] and dynamical hidden orders [36–39].

Up to now the external control of spin-triplet superconductivity has been considered mostly with the help of static fields while several works have studied the effect of magnetization precession on the Josephson current [40–44]. In general, the spin-triplet pairing amplitude $\hat{f}$ can be written in terms of the spin vector [45] $\boldsymbol{d} = (d_x, d_y, d_z)$

$$\hat{f} = (d_x - id_y)|\uparrow\uparrow\rangle + (d_x + id_y)|\downarrow\downarrow\rangle + d_z(|\uparrow\downarrow\rangle + |\downarrow\uparrow\rangle). \quad (1)$$

In this Letter we consider an $S/F/S$ Josephson junction sketched in Fig. 1 with Rashba SOC at the S/F interfaces and demonstrate that external time-dependent electric field produces triplet correlations with the energy and time-dependent spin vector constructed as follows:

$$\boldsymbol{d}(\varepsilon, t) = \int dt' K_d(\varepsilon, t - t')[\boldsymbol{E}(t') \times \boldsymbol{n}] \times \boldsymbol{h}, \quad (2)$$

where $\boldsymbol{n}$ is a normal to the interface plane with Rashba SOC. The scalar kernel $K_d(\varepsilon, t - t')$ is determined below in the framework of a microscopic model. The spin vector $\boldsymbol{d}$ in Eq. (2) is perpendicular to the exchange field $\boldsymbol{h}$ of the ferromagnet. Therefore, according to Eq. (1) it describes superconducting correlations characterized by the spin projections ± 1 on the direction of the exchange field. This shows up through the property of such pairs to be robust to the spin depairing. At the distances $x \gg \xi_F$ only such pairs can survive in the ferromagnet hence named long-range triplets (LRT). Here, ξ_F is the coherence length for opposite-spin pairs in the ferromagnet. In the absence of the electric field only the short-range pairs, which are localized at the coherence length $\xi_F \sim 1$ nm near the superconducting electrodes, are produced, as shown schematically in Fig. 1. Therefore we find the mechanism of electrically stimulated spin-triplet superconductivity, which can support the long-range Josephson current through thick F layer as shown in Figs. 1(b) and 1(c). We suggest that such a system can be

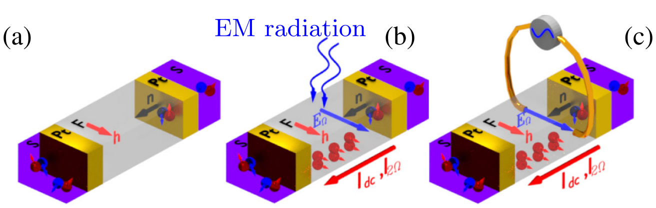

FIG. 1. Schematic picture of the system considered. S/F junction with Rashba SOC at the interface induced by the thin layer of heavy metal Pt. (a) Only short-range superconducting correlations are present shown by the blue and red spheres with opposite arrows. (b),(c) generation of long-range triplet (LRT) correlations due to the irradiation of the setup with electromagnetic wave (b) and by applying the ac current source (c) both producing the electric field $\boldsymbol{E}(t) = \boldsymbol{E}_\Omega e^{i\Omega t}$ in the ferromagnetic interlayer. The LRT are shown schematically by the red spheres with codirected arrows corresponding to the spin states aligned with the exchange field $\boldsymbol{h}$.

considered as the photoactive Josephson junction (JJ). This terminology means that the Josephson current is switched on by the alternating electric field originating, e.g., from the external electromagnetic radiation, as in Fig. 1(b).

Our quantitative calculations are based on the nonstationary version of Usadel-Keldysh theory of superconductivity. The main quantity entering the theory is the pairing amplitude $\check{f}^{R,A} = \hat{f}_s^{R,A} + \boldsymbol{d}^{R,A}\boldsymbol{\sigma}$, which can be written as the sum of spin-singlet $\hat{f}_s^{R,A}$ and spin-triplet $\boldsymbol{d}^{R,A}\boldsymbol{\sigma}$ components. The pairing amplitude in the ferromagnetic part of the structure is described by the linearized Usadel equation

$$\pm iD\partial_x^2 \check{f}^{R,A} = 2\varepsilon \check{f}^{R,A} - \{\boldsymbol{h}\hat{\boldsymbol{\sigma}}, \check{f}^{R,A}\}, \quad (3)$$

where D is the diffusion constant, the $\pm$ sign refers to the retarded (R) and advanced (A) components of the pairing amplitude. The linearized theory is only valid for the weak proximity effect. In our calculation the weakness of the proximity effect is justified by the condition that temperature T is close to the critical temperature T_c. The alternating electric field $\boldsymbol{E}(t) = \sum_i \boldsymbol{E}_{\Omega_i} e^{i\Omega_i t}$ is described by the time-dependent vector potential $\boldsymbol{E} = -\partial_t \boldsymbol{A}/c$. We assume that $p_{s,i}\xi_{\Omega_i} \ll 1$ and $p_{s,i}\xi_S \ll 1$, where $p_{s,i} = 2eE_{\Omega_i}/\Omega_i$ is the absolute value of the condensate momentum at a given frequency, $\xi_S = \sqrt{D/\Delta}$ and $\xi_{\Omega_i} = \sqrt{D/\Omega_i}$ are the coherence lengths in the superconductor and the nonsuperconducting metal, respectively. Then the small terms $\propto \boldsymbol{A}_{\Omega_i}\boldsymbol{A}_{\Omega_j}$, which are not spin active and do not lead to any singlet-triplet or short-range-triplet–long-range-triplet conversion, are neglected in Eq. (3). For the spin-singlet component there is a usual Kupriyanov-Lukichev boundary condition [46]

$$(\boldsymbol{n}\boldsymbol{\nabla})\hat{f}_s^{R,A} = \gamma \hat{F}_{bcs}^{R,A}, \quad (4)$$

where γ is the S/F interface conductance, $\hat{F}_{bcs}^{R,A} = \mp \tau_3 \hat{\Delta}/(\varepsilon \pm i\delta)$ and $\hat{\Delta} = |\Delta(x)| \exp[i\chi(x)\hat{\tau}_3]\hat{\tau}_1$. We assume $|\Delta(x)| = 0$ in the interlayer of the Josephson junction $-d_F/2 \le x \le d_F/2$, while $|\Delta(x)| = \Delta$ and $\chi(x) = \mp \chi/2$ is the superconducting phase in the left (right) leads. $\hat{\tau}_i$ and $\hat{\sigma}_i$ are Pauli matrices in particle-hole and spin spaces, respectively, and $\hat{\boldsymbol{\sigma}} = (\hat{\sigma}_1, \hat{\sigma}_2, \hat{\sigma}_3)^T$.

The presence of Pt layer is modeled by the Rashba constant $\alpha(x)$ which is only nonzero in the restricted region near the S/F interface. We introduce $\tilde{\alpha} = \int dx \alpha(x)$ as the surface SOC strength and obtain the boundary condition for the spin-triplet component [47], which is our first main result

$$(\boldsymbol{n}\boldsymbol{\nabla})\boldsymbol{d}^{R,A} = \frac{4ie}{c}\tilde{\alpha}\hat{\tau}_3 \sum_i e^{i\Omega_i t}(\boldsymbol{A}_{\Omega_i} \times \boldsymbol{n}) \times \left[\boldsymbol{d}^{R,A}\left(\varepsilon + \frac{\Omega_i}{2}\right) + \boldsymbol{d}^{R,A}\left(\varepsilon - \frac{\Omega_i}{2}\right)\right]. \quad (5)$$

In general the solution of Eq. (3) consists of short-range and long-range modes. They decay in the ferromagnetic region at the distances of $\xi_F = \sqrt{D/h}$ and ξ_{Ω_i}, respectively. Solving Eqs. (3)–(5) for the Josephson setups Figs. 1(b) and 1(c) we obtain [47] the LRT:

$$\boldsymbol{d}^{R,A}(\varepsilon, t) = \sum_j \boldsymbol{d}^{R,A}_{\Omega_j}(\varepsilon) e^{i\Omega_j t}, \quad (6)$$

with

$$\boldsymbol{d}^{R,A}_{\Omega}(\varepsilon) = K^{R,A}_d(\varepsilon, \Omega)[(\boldsymbol{E}_\Omega \times \boldsymbol{n}) \times \boldsymbol{h}], \quad (7)$$

which is our second main result. The kernel in Eq. (7) in the limit $\xi_F \ll d_F \ll \xi_{\Omega_i}$ takes the form

$$K^{R,A}_d(\varepsilon, \Omega) = \pm \frac{4e\tilde{\alpha}\xi_F^2(\gamma\xi_F)|\Delta|\sin(\chi/2)\hat{\tau}_2}{d_F[(\varepsilon \pm i\delta)^2 - (\Omega/2)^2]\Omega}. \quad (8)$$

The qualitative physical picture of the LRT's generation in Eq. (5) is determined by the hidden p-wave correlations which are induced by the interplay of SOC and exchange field $\boldsymbol{h}$ at the S/F interface and the p-wave to s-wave conversion induced by the electric field drive. First, we recall that the spin splitting by the exchange field near the S/F interface [48–51] provides the spin mixing and thus induces the s-wave spin-triplet superconducting correlations $\boldsymbol{d}^{\rm short}_{sw} = (i\gamma\xi_F F_{bcs}/2h)\boldsymbol{h}$ with zero spin projections $S_z = 0$ on the quantization axis $\|\boldsymbol{h}$, where $F^{R,A}_{bcs} = \mp \Delta/(\varepsilon \pm i\delta)$. These correlations are short-ranged in the ferromagnet. The SOC does not provide spin splitting (neglecting the small terms of the order of α/v_F, where v_F is the Fermi velocity), but it induces the momentum-dependent rotation of the spin quantization axis $\boldsymbol{h} \to \boldsymbol{h} + \alpha\boldsymbol{n} \times \boldsymbol{p}$ where $\boldsymbol{p}$ is the electron momentum. This provides a conversion of the spin-triplet s-wave $\boldsymbol{d}^{\rm short}_{sw}$ to the spin-triplet p-wave $\boldsymbol{d}_{pw}$ correlations. This conversion follows from the standard quasiclassical Eilenberger equation in the presence of SOC. In the diffusive limit it yields a general local relation $\boldsymbol{d}_{pw} = i(D\alpha/p)(\boldsymbol{p} \times \boldsymbol{n}) \times \boldsymbol{d}^{\rm short}_{sw}$, see Fig. 2(a). Similar mechanisms of the triplet p-wave component generation take place in various topological superconductivity platforms.

Thus spin-triplet correlations are characterized by the spin vector $\boldsymbol{d}_{pw}(\boldsymbol{p}, \varepsilon) = F_{pw}(\varepsilon)\boldsymbol{h} \times (\boldsymbol{n} \times \boldsymbol{p})$ with the amplitude $F_{pw}(\varepsilon) = i\alpha\gamma D\xi_F F_{bcs}/2hp$. The p-wave pairing exists only in the surface layer with nonzero SOC $\alpha(x) \neq 0$. Outside this layer it vanishes at the mean free path length and therefore does not penetrate into the ferromagnet. However, the electric field induces the condensate momentum $\boldsymbol{p}_s = -2ie\boldsymbol{E}_\Omega/\Omega$ providing coupling between orbital p-wave and s-wave components via the added energy Doppler shift [52,53] $\boldsymbol{p} \cdot \boldsymbol{p}_s/m$. As a result the amplitude of triplet correlations is given by

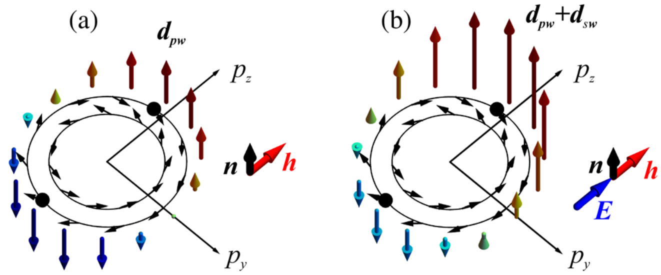

FIG. 2. Mechanism behind the formation of spin-triplet superconducting correlations. Helical Fermi surface cross sections $p_x = 0$ in the region close to S/F interface with Rashba SOC and exchange field. Local directions of spin quantization axes are marked by black arrows. Small black spheres show states with opposite momenta $\boldsymbol{p}$ and $-\boldsymbol{p}$. Rashba SOC vector is $\boldsymbol{n} = \boldsymbol{x}$ and exchange field $\boldsymbol{h} = h\boldsymbol{z}$. (a) Noncollinearity of spins at $\boldsymbol{p}$ and $-\boldsymbol{p}$ results in the spin-triplet pairing with p-wave spin vector $\boldsymbol{d}_{pw} \propto (\boldsymbol{n} \times \boldsymbol{p}) \times \boldsymbol{h} \| \boldsymbol{x}$. (b) Alternating electric field $\boldsymbol{E}$ shown by the blue arrow results in the mixing between p- and s-wave pairing amplitudes.

$F_{pw}(\varepsilon + \boldsymbol{p}\cdot\boldsymbol{p}_s/m) \approx F_{pw}(\varepsilon) + (\boldsymbol{p}\cdot\boldsymbol{p}_s/m)\partial_\varepsilon F_{pw}$. This modification of the pairing amplitude produces the additional s-wave component of the spin vector $\boldsymbol{d}^{\rm long}_{sw} \propto \boldsymbol{h} \times (\boldsymbol{n} \times \boldsymbol{E})$ with spin projections $S_z = \pm 1$ on the quantization axis, which is suppressed neither by the impurity scattering nor by the exchange field. The vector field $\boldsymbol{d} = \boldsymbol{d}_{pw} + \boldsymbol{d}^{\rm long}_{sw}$ is shown schematically in Fig. 2(b). As a result we obtain the conversion of s-wave $S_z = 0$ to the s-wave $S_z = \pm 1$ pairs through the local p-wave correlations and the Doppler shift. On the level of Usadel equations, which only operate with s-wave Green's functions, this three-stage process results in the nonzero rhs of the boundary conditions (5).

Photo-induced Josephson current.—The overlapping between two LRT amplitudes penetrating from the both S/F interfaces gives rise to the nonzero Josephson effect. For the case of a harmonic electromagnetic wave we get the current-phase relation

$$I(\chi, t) = [I^c_{\rm dc} + I^c_{2\Omega}\cos(2\Omega t)]\sin\chi. \quad (9)$$

Note that here both the dc and double-frequency critical current amplitudes are determined by the alternating electric field $I^c_{\rm dc} \propto E_\Omega E_{-\Omega}$ and $I^c_{2\Omega} \propto E^2_\Omega$. The particular values of the critical currents $I^c_{\rm dc}$, $I^c_{2\Omega}$ can be found in the Supplemental Material [47]. By the order of magnitude $I^c_{\rm dc}$, $I^c_{2\Omega} \sim I_0$, where

$$I_0 = -\sigma_F S(\Delta/ed_F)(2\tilde{\alpha}\gamma\xi_F/\pi)^2(\Delta/T)^2 P/P_c, \quad (10)$$

where S is the junction area, $P = c|E_\Omega|^2$ is the radiation power, $P_c = (c\hbar/e^2)\hbar\Omega^2/\xi_S^2$ is the radiation power needed to speed up the Cooper pairs to the depairing velocity. The scale I_0 can be estimated using the typical parameters of JJ with ferromagnetic interlayers [54]: the junction area is

$50 \times 50\ \mu\mathrm{m}^2$, $\sigma_F \sim (50\ \mu\Omega\,\mathrm{cm})^{-1}$, $d_F \sim \gamma^{-1} \sim 5\xi_F$, and $D \sim 10\ \mathrm{cm}^2/\mathrm{s}$, $h \sim 500$ K so that $\xi_F \sim 3$ nm. For the superconducting gap in Nb $\Delta \sim 10$ K so that the critical current is $I_0 \sim 10^{-1}(p_s\xi_S)^2\tilde{\alpha}^2$ A. Taking $\tilde{\alpha} \sim 0.1$–1 [15, 55–58] we get the current $I_0/(p_s\xi_S)^2 \sim 10^{-1} - 10^{-3}$ A. Given that $\xi_S \approx 30$ nm we get $P_c \approx 10\ (\Omega/\mathrm{GHz})^2\ \mathrm{W/m}^2$. Therefore such a JJ is quite sensitive to the radio-frequency and microwave irradiation. A typical cell phone at one meter distance generates microwave radiation with $\Omega \approx$ 3–4 GHz and $P \sim P_c$ which induces rather large currents $I_0 \sim 10^{-1} - 10^{-3}$ A. At the same time the power sensitivity strongly decreases with the frequency rise. For the frequency corresponding to the cosmic background radiation $P_c \approx 10^6\ \mathrm{W/m}^2$ so that the power density $P = 10^{-5}\ \mathrm{W/m}^2$ induces rather small critical current $I_0 \sim 10^{-12} - 10^{-15}$ A. Still, it is possible to induce large critical current using terahertz and visible light radiation sources. The 1 THz radiation with power 1 $\mathrm{mW/mm}^2$ yields $I_0 \sim 10^{-5} - 10^{-7}$ A. Laser beam of the frequency about $\Omega \sim 10^6$ GHz carrying the power 1 mW focused into the spot of 1 $\mu\mathrm{m}^2$ size induces the critical current $I_0 \sim 10^{-6} - 10^{-8}$ A which is well within the measurable limits.

In IV characteristics of conventional Josephson junctions Shapiro steps can be observed at $2\ \mathrm{eV} = \hbar n\Omega$ under periodic external perturbations: a periodic applied current or under irradiation. For the system under consideration the driving electric field is parallel to the interfaces and thus does not induce the voltage across the junction. This geometry is qualitatively different from the usual experiments on microwave-induced Shapiro steps. Nevertheless, the presence of the second harmonic contribution to the critical Josephson current (9) leads to the Shapiro steps with unusual properties even under a constant applied current. For the system under consideration the Shapiro steps take place at voltages $2\ \mathrm{eV} = 2\hbar n\Omega$. That is only the even-numbered Shapiro steps show up in the photoactive JJ. Obviously, it is a consequence of the fact that the ac component of the current oscillates with a frequency twice larger than the externally applied source. The second essential difference with the conventional case is that the value of the critical current grows with the radiation power, as it is demonstrated by different curves in Fig. 3(a). This is a signature of the irradiation-induced LRT correlations.

Josephson photomagnetic devices.—Electric-field induced current across the JJ, described by Eqs. (9) and (10), provides an interesting possibility to create photomagnetic devices based on the superconducting loops with the weak links formed by the radiation-controlled JJ. We show that applying the radiation as it is shown in the schematic Fig. 3(b), it is possible to generate spontaneous currents circulating in the loop, which in turn produce a dc component of the magnetic field $\boldsymbol{B}_{\mathrm{dc}}$.

We consider a dc SQUID with one of the branches connected by photoactive JJ and the other by a π-JJ which

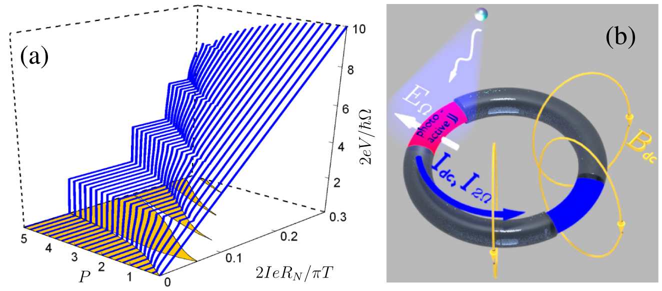

FIG. 3. (a) IV characteristics of the irradiated photoactive JJ at a constant applied current I. Different blue curves correspond to different values of the applied radiation power $P = 2eR_N I^c_{\mathrm{dc}}/(\hbar\Omega)$ at a given frequency, R_N is the JJ resistance in the normal state. $\hbar\Omega/\pi T = 0.03$. Shown with yellow shadings are the domains in (I, P) plane with constant voltage generated across the JJ. (b) Schematic picture of the photomagnetic SQUID. The device consists of the photoactive Josephson junction (red weak link) and the usual JJ (blue weak link). Electric field $\boldsymbol{E}_\Omega e^{i\Omega t}$ from the incoming radiation switches on both dc I_{dc} and $I_{2\Omega}e^{2i\Omega t}$ components of the circulating current. The dc component produces spontaneous magnetic field $\boldsymbol{B}_{\mathrm{dc}}$.

is used as a passive phase shifter element as in the "quiet" superconducting qubits proposals [59–61] and rapid single flux quantum logic devices [62]. Dynamics of Josephson phases χ_1 across the photoactive JJ and χ_2 across the π-JJ is determined by the system of coupled sine-Gordon equations [63], which is similar to the one used for the standard dc SQUID. The essentially different effects are determined by the two factors. The first one is the possibility of various parametric effects due to the time-dependent current amplitude in the photoactive JJ. These effects can be expected for the frequencies comparable with the eigenfrequency of the superconducting loop $\omega_0 = 1/\sqrt{LC}$. Here, we consider the opposite case when $\Omega \ll \omega_0$ and use the second nontrivial property of the system, which is the critical current of the photoactive JJ controllable by the radiation power. In this case we can separate the timescales corresponding to rapid oscillations and slow period-averages drift described by the coordinate $\boldsymbol{\chi} = (\bar{\chi}_1, \bar{\chi}_2)$ where $\bar{\chi}_k = \Omega\int_0^{\Omega^{-1}} \chi_k dt$. In the absence of external irradiation there are no currents and phase differences are $\bar{\chi}_{1,2} = 0$. Radiation switches on the photoactive JJ. Then gradually increasing the radiation power we get that the zero-current state becomes unstable under the following condition [47]:

$$I^c_{\mathrm{dc}} > \frac{\Phi_0}{2\pi}\frac{\omega_0\omega_p}{\sqrt{\omega_0^2 + \omega_p^2}}, \qquad (11)$$

where $\omega_p = \sqrt{2\pi I^c_\pi/C\Phi_0}$ is the plasma frequency corresponding to the π-JJ. In case of the typical values $\omega_p = \omega_0 \sim 10$ GHz we get the threshold value in the rhs of Eq. (11) about 10^{-6} A.

Once the condition (11) is satisfied the SQUID switches to the state with spontaneous dc current $I_{\rm dc}$ and constant magnetic field $\boldsymbol{B}_{\rm dc}$ shown schematically in Fig. 3(b). The photoinduced magnetic flux magnitude can be estimated as $LI^c_{\rm dc}$. For the typical values of the SQUID loop inductance $L \approx 10^{-11}$ H and $I^c_{\rm dc} \approx 10^{-6}$ A we get the flux of $10^{-2}\Phi_0$.

One can obtain the photomagnetic response without any threshold for the incoming power provided the second branch of the SQUID contains the Josephson phase battery [14,64–66] based on the JJ with shifted current-phase relation $I = I^c_\varphi \sin(\chi - \varphi_0)$ with $\varphi_0 \neq \pi n$. Such a photomagnetic element generates dc current $I_{\rm dc} \approx I^c_{\rm dc} \cos\varphi_0$ and the corresponding magnetic field $\boldsymbol{B}_{\rm dc}$ being exposed to any arbitrary small radiation power.

In conclusion, we have demonstrated the possibility of generating dynamic spin-triplet superconducting order which emerges under nonequilibrium conditions induced by the alternating electric field. Qualitatively the obtained effect arises due to the partial conversion of the p-wave triplet superconductivity, taking place in the presence of the Rashba SOC and ferromagnetism, to the s-wave odd-frequency triplet correlations. The conversion is caused by the Doppler shift of the quasiparticle spectrum induced by the nonstationary condensate motion under the action of the electric field. The detailed qualitative discussion and development of the microscopic model of this mechanism are provided. We propose a scheme of a Josephson transistor which can be switched by the ac current and a photomagnetic SQUID, which generates magnetic fields under irradiation.

The work of M. A. S was supported by the Academy of Finland (Project No. 297439) and Russian Science Foundation, Grant No. 20-12-00053. The work of I. V. B and A. M. B has been carried out within the state task of ISSP RAS with the support by RFBR Grants No. 19-02-00466, No. 18-52-45011, and No. 18-02-00318. I. V. B. also acknowledges the financial support by Foundation for the Advancement of Theoretical Physics and Mathematics BASIS.

[1] T. Clark, R. Prance, and A. Grassie, J. Appl. Phys. **51**, 2736 (1980).
[2] K. K. Likharev and V. K. Semenov, IEEE Trans. Appl. Supercond. **1**, 3 (1991).
[3] T. W. Larsen, K. D. Petersson, F. Kuemmeth, T. S. Jespersen, P. Krogstrup, J. Nygård, and C. M. Marcus, Phys. Rev. Lett. **115**, 127001 (2015).
[4] L. Casparis, T. W. Larsen, M. S. Olsen, F. Kuemmeth, P. Krogstrup, J. Nygård, K. D. Petersson, and C. M. Marcus, Phys. Rev. Lett. **116**, 150505 (2016).
[5] A. F. Volkov, Phys. Rev. Lett. **74**, 4730 (1995).
[6] A. Morpurgo, T. Klapwijk, and B. Van Wees, Appl. Phys. Lett. **72**, 966 (1998).
[7] J. Baselmans, A. Morpurgo, B. Van Wees, and T. Klapwijk, Nature (London) **397**, 43 (1999).
[8] J. Huang, F. Pierre, T. T. Heikkilä, F. K. Wilhelm, and N. O. Birge, Phys. Rev. B **66**, 020507(R) (2002).
[9] F. Paolucci, F. Vischi, G. De Simoni, C. Guarcello, P. Solinas, and F. Giazotto, Nano Lett. **19**, 6263 (2019).
[10] G. De Simoni, F. Paolucci, P. Solinas, E. Strambini, and F. Giazotto, Nat. Nanotechnol. **13**, 802 (2018).
[11] Y.-J. Doh, J. A. van Dam, A. L. Roest, E. P. Bakkers, L. P. Kouwenhoven, and S. De Franceschi, Science **309**, 272 (2005).
[12] S. Abay, D. Persson, H. Nilsson, F. Wu, H. Q. Xu, M. Fogelström, V. Shumeiko, and P. Delsing, Phys. Rev. B **89**, 214508 (2014).
[13] J. A. Van Dam, Y. V. Nazarov, E. P. Bakkers, S. De Franceschi, and L. P. Kouwenhoven, Nature (London) **442**, 667 (2006).
[14] D. Szombati, S. Nadj-Perge, D. Car, S. Plissard, E. Bakkers, and L. Kouwenhoven, Nat. Phys. **12**, 568 (2016).
[15] C. R. Ast, J. Henk, A. Ernst, L. Moreschini, M. C. Falub, D. Pacilé, P. Bruno, K. Kern, and M. Grioni, Phys. Rev. Lett. **98**, 186807 (2007).
[16] G. Bihlmayer, Y. M. Koroteev, P. Echenique, E. Chulkov, and S. Blügel, Surf. Sci. **600**, 3888 (2006).
[17] A. Manchon, H. C. Koo, J. Nitta, S. Frolov, and R. Duine, Nat. Mater. **14**, 871 (2015).
[18] N. H. Lindner, G. Refael, and V. Galitski, Nat. Phys. **7**, 490 (2011).
[19] J. Cayao, C. Triola, and A. M. Black-Schaffer, Phys. Rev. B **103**, 104505 (2021).
[20] F. Wilczek, Phys. Rev. Lett. **111**, 250402 (2013).
[21] N. Y. Yao, A. C. Potter, I.-D. Potirniche, and A. Vishwanath, Phys. Rev. Lett. **118**, 030401 (2017).
[22] S. Autti, V. B. Eltsov, and G. E. Volovik, Phys. Rev. Lett. **120**, 215301 (2018).
[23] C. Triola, A. Pertsova, R. S. Markiewicz, and A. V. Balatsky, Phys. Rev. B **95**, 205410 (2017).
[24] H. Hübener, M. A. Sentef, U. De Giovannini, A. F. Kemper, and A. Rubio, Nat. Commun. **8**, 13940 (2017).
[25] M. A. Sentef, M. Claassen, A. F. Kemper, B. Moritz, T. Oka, J. K. Freericks, and T. P. Devereaux, Nat. Commun. **6**, 7047 (2015).
[26] D. Fausti, R. Tobey, N. Dean, S. Kaiser, A. Dienst, M. C. Hoffmann, S. Pyon, T. Takayama, H. Takagi, and A. Cavalleri, Science **331**, 189 (2011).
[27] M. Claassen, D. M. Kennes, M. Zingl, M. A. Sentef, and A. Rubio, Nat. Phys. **15**, 766 (2019).
[28] J. Tindall, F. Schlawin, M. Buzzi, D. Nicoletti, J. R. Coulthard, H. Gao, A. Cavalleri, M. A. Sentef, and D. Jaksch, Phys. Rev. Lett. **125**, 137001 (2020).
[29] M. Budden, T. Gebert, M. Buzzi, G. Jotzu, E. Wang, T. Matsuyama, G. Meier, Y. Laplace, D. Pontiroli, M. Riccò, F. Schlawin, D. Jaksch, and A. Cavalleri, Nat. Phys. **17**, 611 (2021).
[30] M. Mitrano, A. Cantaluppi, D. Nicoletti, S. Kaiser, A. Perucchi, S. Lupi, P. Di Pietro, D. Pontiroli, M. Riccò, S. R. Clark, D. Jaksch, and A. Cavalleri, Nature (London) **530**, 461 (2016).
[31] M. A. Sentef, A. F. Kemper, A. Georges, and C. Kollath, Phys. Rev. B **93**, 144506 (2016).

[32] T. Yu, M. Claassen, D. M. Kennes, and M. A. Sentef, Phys. Rev. Research **3**, 013253 (2021).

[33] T. Yokoyama, J. Phys. Soc. Jpn. **89**, 103703 (2020).

[34] S. V. Mironov, A. S. Melnikov, I. D. Tokman, V. Vadimov, B. Lounis, and A. I. Buzdin, Phys. Rev. Lett. **126**, 137002 (2021).

[35] Y. Ashida, A. m. c. İmamoğlu, J. Faist, D. Jaksch, A. Cavalleri, and E. Demler, Phys. Rev. X **10**, 041027 (2020).

[36] A. V. Balatsky, P. O. Sukhachov, and S. Bandyopadhyay, Ann. Phys. (Berlin) **532**, 1900529 (2020).

[37] J. Linder and A. V. Balatsky, Rev. Mod. Phys. **91**, 045005 (2019).

[38] G. Aeppli, A. V. Balatsky, H. M. Rønnow, and N. A. Spaldin, Nat. Rev. Mater. **5**, 477 (2020).

[39] L. Stojchevska, I. Vaskivskyi, T. Mertelj, P. Kusar, D. Svetin, S. Brazovskii, and D. Mihailovic, Science **344**, 177 (2014).

[40] J.-X. Zhu, Z. Nussinov, A. Shnirman, and A. V. Balatsky, Phys. Rev. Lett. **92**, 107001 (2004).

[41] M. Houzet, Phys. Rev. Lett. **101**, 057009 (2008).

[42] A. F. Volkov and K. B. Efetov, Phys. Rev. Lett. **103**, 037003 (2009).

[43] C. Holmqvist, S. Teber, and M. Fogelström, Phys. Rev. B **83**, 104521 (2011).

[44] T. Yokoyama and Y. Tserkovnyak, Phys. Rev. B **80**, 104416 (2009).

[45] A. J. Leggett, Rev. Mod. Phys. **47**, 331 (1975).

[46] M. Y. Kuprianov and V. F. Lukichev, Zh. Eksp. Teor. Fiz. **94**, 139 (1988) [Sov. Phys. JETP **67**, 1163 (1988)].

[47] See Supplemental Material at http://link.aps.org/supplemental/10.1103/PhysRevLett.127.147701 for the detailed derivation of the the boundary conditions Eq. (5), solution for the dynamic spin-triplet order Eqs. (7,8) and the Josephson current Eq. (9).

[48] F. S. Bergeret, A. F. Volkov, and K. B. Efetov, Rev. Mod. Phys. **77**, 1321 (2005).

[49] A. I. Buzdin, Rev. Mod. Phys. **77**, 935 (2005).

[50] J. Linder and J. W. A. Robinson, Nat. Phys. **11**, 307 (2015).

[51] M. Eschrig, A. Cottet, W. Belzig, and J. Linder, New J. Phys. **17**, 083037 (2015).

[52] W. V. Budzinski, M. P. Garfunkel, and R. W. Markley, Phys. Rev. B **7**, 1001 (1973).

[53] A. Kohen, T. Proslier, T. Cren, Y. Noat, W. Sacks, H. Berger, and D. Roditchev, Phys. Rev. Lett. **97**, 027001 (2006).

[54] Y. V. Fominov, A. F. Volkov, and K. B. Efetov, Phys. Rev. B **75**, 104509 (2007).

[55] S.-T. Lo, S.-W. Lin, Y.-T. Wang, S.-D. Lin, and C.-T. Liang, Sci. Rep. **4**, 5438 (2014).

[56] N. Banerjee, J. A. Ouassou, Y. Zhu, N. A. Stelmashenko, J. Linder, and M. G. Blamire, Phys. Rev. B **97**, 184521 (2018).

[57] C. Triola, D. M. Badiane, A. V. Balatsky, and E. Rossi, Phys. Rev. Lett. **116**, 257001 (2016).

[58] J. Cayao and A. M. Black-Schaffer, Phys. Rev. B **98**, 075425 (2018).

[59] L. B. Ioffe, V. B. Geshkenbein, M. V. Feigel'Man, A. L. Fauchere, and G. Blatter, Nature (London) **398**, 679 (1999).

[60] G. Blatter, V. B. Geshkenbein, and L. B. Ioffe, Phys. Rev. B **63**, 174511 (2001).

[61] A. Feofanov, V. Oboznov, V. BolGinov, J. Lisenfeld, S. Poletto, V. Ryazanov, A. Rossolenko, M. Khabipov, D. Balashov, A. Zorin *et al.*, Nat. Phys. **6**, 593 (2010).

[62] A. Ustinov and V. Kaplunenko, J. Appl. Phys. **94**, 5405 (2003).

[63] A. Barone and G. Paterno, *Physics and Applications of the Josephson Effect* (Wiley, New York, 1982).

[64] A. Buzdin, Phys. Rev. Lett. **101**, 107005 (2008).

[65] A. Assouline, C. Feuillet-Palma, N. Bergeal, T. Zhang, A. Mottaghizadeh, A. Zimmers, E. Lhuillier, M. Eddrie, P. Atkinson, M. Aprili *et al.*, Nat. Commun. **10**, 126 (2019).

[66] E. Strambini, A. Iorio, O. Durante, R. Citro, C. Sanz-Fernández, C. Guarcello, I. V. Tokatly, A. Braggio, M. Rocci, N. Ligato, V. Zannier, L. Sorba, F. S. Bergeret, and F. Giazotto, Nat. Nanotechnol. **15**, 656 (2020).